Effects of in-plane straining on the out-of-plane delamination properties of paperboard

ULF STIGH, ANDERS BIEL, JOHAN TRYDING, MIKAEL NYGÅRDS, HANNES VOMHOFF, CAMILLA PERSSON, CHRISTER KORIN, AND PATRIK KARLSSON

ABSTRACT: Delamination strength is an essential property for the creasing and folding operations of paperboard into boxes. Due to fixation during creasing, the paperboard suffers in-plane straining. In the present study, we aim to increase our understanding of how in-plane straining affects the delamination properties of paperboard.

Samples of paperboard were first strained in in-plane tensile loading, both in the machine-direction and in the cross-direction. Afterward, the paperboard is loaded in the out-of-plane (ZD) direction. Three different grades of commercial paperboard from two major manufacturers were tested in a climate-controlled lab. The results showed similar results for all grades of paperboard, with the delamination strength and the out-of-plane stiffness decreasing virtually linearly with pre-straining. With about 5% plastic in-plane straining, the strength was reduced by about 20% and the stiffness decreased by more than 50% for all grades of paperboard. Normalizing the strength and the stiffness with their values without pre-straining reveals virtually the same relation for all grades of paperboard. If proven to be a general result, this will prove valuable in reducing the demand for experiments.

Application: The results from this study are important for the understanding and modeling of creasing and folding of paperboard.

The industrial relevance of understanding how in-plane pre-straining affects out-of-plane delamination is substantial. During creasing and folding, fixtures and toolpaths impose in-plane stretching that can reduce z-direction stiffness and strength. Quantifying these effects enables manufacturers to adjust crease design, fixation, and folding parameters to minimize surface cracking. An authoritative review of the development of the creasing and folding technology from prehistoric times to the present day is given in [1].

During the creasing process, the paperboard delaminates in the crease line. Here, the paperboard is divided into thinner plies. Each of these plies is thinner than the original paperboard, as illustrated in **Fig. 1**. During the subsequent folding process, the paperboard is bent. During bending, the inner layers are compressed, and the outer plies are pulled. That is, compressive in-plane stressing occurs in the inner plies of the fold. These stresses lead to local buckling of the compressed layers. This helps to form a permanent fold line. Tensile in-plane stresses in the outer plies of the fold balance the compressive stresses of the inner plies. If too large in-plane tensile stresses develop during folding, cracks may develop on the outside of the box at the fold line. Cracks on the outside surfaces should be avoided.

The buckling stress depends on the thickness and length of the compressed inner ply (for elastic buckling, the buckling stress scales with the square of the thickness of the compressed layer and the square of the length of the de-

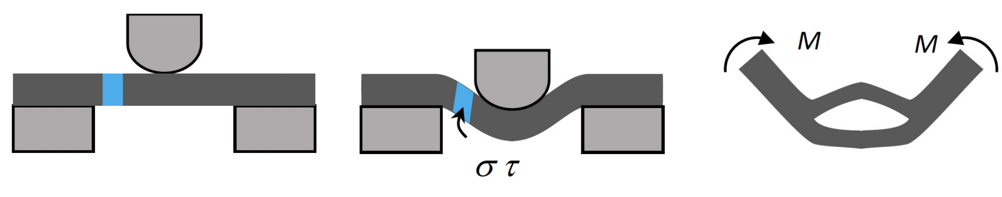

1. Principle of creasing and folding. Left: Paperboard (dark gray) positioned over a matrix (lower light grey boxes). The creasing ruler is sketched as the upper light gray semicircular object. The blue area in the paperboard is used to visualize the straining during creasing. Middle: The ruler is pressed vertically into the paperboard, resulting in a crease line. During the process, out-of-plane stresses develop; opening stress σ, due to the vertical stretching of the paperboard, and shear stresses τ, due to the out-of-plane shearing of the paperboard. This results in delamination cracks. Right: In the subsequent folding process, the inner delaminated layers buckle, and the outer delaminated layers are stretched as the paperboard is bent.

laminated layer [2]), and surface cracks are driven by the balancing tensile stresses acting on the outer ply. Thus, the processes involved for creasing and folding need to be well-understood for an optimization of the converting process. Numerical simulations are being developed to improve the creasing process. The success of these models critically depends on the material model used and the accuracy of the constitutive properties used in the models. To date, constitutive properties have to be measured experimentally. Studies of the mechanics of paperboard related to creasing and folding, from a modeling, numerical, and/or experimental perspective, are found in [1,3-13]. Micromechanical studies aiming at increasing our understanding of the nonlinear properties of paperboard are presented in [14-19].

Delamination cracks in paperboard are primarily caused by the out-of-plane (ZD) stresses and the compressive in-plane stresses. The out-of-plane stresses are both opening and shear stresses. Studies of the mechanical out-of-plane properties of paperboard are conducted by bonding the paperboard to metal substrates that are mounted in the grips of a tensile test machine. The grips of the test machine are gradually separated, and the separation and applied force are measured. Traditional methods assume a uniform stress field in the paperboard. By this assumption, stress-separation data is recorded. The stress first increases nearly linearly with increasing separation of the surfaces of the paperboard. That is, the response is initially elastic, and upon unloading, the paperboard almost returns to its initial, virgin state. However, at a certain stress level, denoted the out-of-plane strength, delamination cracks nucleate at weak spots in the paperboard. As the separation is further increased, the stress decreases as the cracks widen. At a final state, the crack faces span the complete paperboard, and the stress is zero.

Figure 2 illustrates the experimental setup used in a standardized method (TAPPI Standard Test Method T 541 “Internal bond strength of paperboard [z-direction tensile]”) for separation tests in the opening direction; that is, resulting in an opening stress. The test method is described later in more detail in the “ZD tests” portion of the Experimental section. For shear testing, corresponding methods have to date been unsuccessful in achieving stable tests. That is, before the paperboard is completely separated into two plies, the paperboard suddenly splits into two plies due to the instability of the test setup.

In the context of delamination, the shear-mode strength is several times larger than the opening-mode strength. For the paperboards studied here, the shear delamination strength is about four times the opening strength. In contrast, the critical separation at complete delamination in the shear mode is roughly one quarter of that in the opening mode. This puts higher demands on the test procedures in shear than in opening mode separation. In shear, the tests are prone to terminate prematurely due to instability. A recently presented novel test procedure enables stable

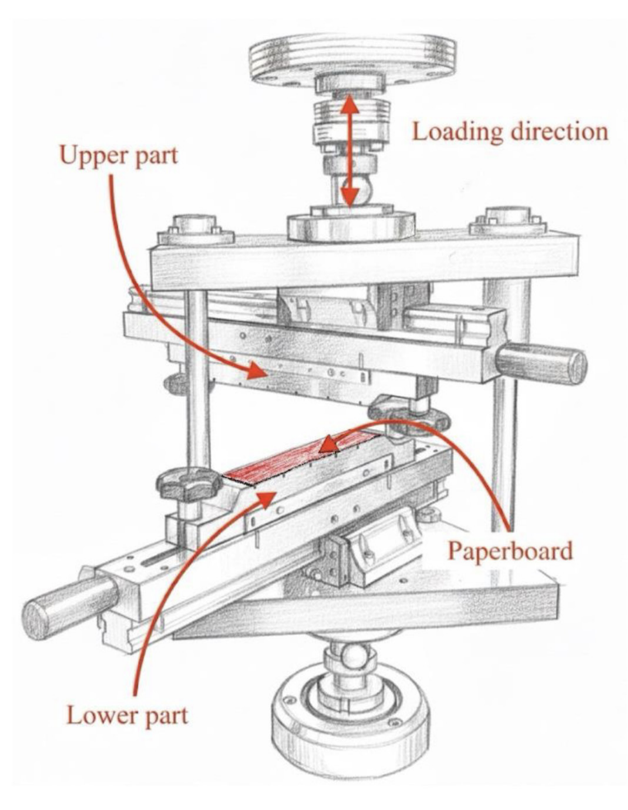

2. Test setup for delamination tests in ZD (out-of-plane) for tests according to TAPPI T 541. The principal sketch illustrates the setup before the ZD-test. At this moment, the paperboard (red area) is attached to the lower part of the rig. In the next step, the upper part of the rig is moved downwards, and the pressure-sensitive adhesive (PSA) on the upper part is pressed onto the paperboard. After a short dwell time, the upper part is moved upward in the loading direction, and the ZD-test is performed.

shear testing [20]. This procedure is currently optimized for ease of handling [21].

Fixation of the paperboard during creasing prevents the paperboard from slipping in its plane and thus secures an accurate positioning of the crease line on the paperboard. However, the fixation also results in in-plane straining of the paperboard; the paperboard has to follow the deformed path by the creasing ruler and matrix (Fig. 1). This stretches the paperboard in its plane. An estimate based on a simple geometrical model gives in-plane strains of the order of 10% during creasing. The estimate is based on calculating the length of a surface element in its creased and non-creased states using a reasonable geometry for creasing as in Fig. 1. The actual level is determined by the precise design of the fixation mechanism that locks the paperboard before it is creased. Potential effects of this straining are not considered in current models of converting processes (see, for example, [11,12]).

In the present study, we aim to show that in-plane straining reduces the ZD stiffness and strength. This is done by measuring the properties of the paperboard in its out-of-

Property	B315	B290	H330
Thickness, µm	485	415	440
Grammage, g/m²	307	298	325
Number of plies	4	3	3

I. Paperboard qualities and measured data.

plane direction in the virgin state of the paperboard and in different levels of in-plane straining.

MATERIALS

Three grades of commercial paperboard are used in the present study. These are designated as B315, B290, and H330. Here, the number indicates the nominal grammage in grams per square meter (g/m²) of the paperboard, as shown **Table I**. These paperboards are chosen because they have similar thickness and grammage but represent a significant variation in production methods. They are made on three different paperboard machines and are produced as three- or four-ply sheets. The B315 is a duplex board, while the other two are bleached boards. All are pigment coated, with multiple plies that have different properties to suit various commercial uses. The B315 and the B290 have outer plies made of kraft fiber and inner plies of a mix of chemithermomechanical pulp (CTMP), broke, and kraft fibers. Similarly, H330 consists of outer plies of kraft fibers, with the inner ply made from a blend of kraft and broke fibers. With this background, we can measure variations in properties. The paperboards were delivered as 210 mm x 297 mm (A4 size) sheets with the long side in the machine-direction (MD). Before testing, the sheets were conditioned in a climate-controlled laboratory for several days. The lab is maintained at 23°C and 50% relative humidity. The sheets are first measured for thickness and grammage. The data are summarized in Table I.

EXPERIMENTAL

To identify the effects of in-plane straining, the paperboard is strained using tensile loading. That is, the paperboard is stretched to different levels of strain. This is done both in the MD and in the cross-direction (CD). This process produces damaged samples of paperboard that are loaded in the z-direction in the final step. Thus, the experiments are performed in two steps:

- Step 1. *In-plane tensile loading of the paperboard* in both MD and CD. This creates paperboard with varying levels of damage, which is used in the subsequent delamination tests. The tensile tests are either run until the paperboard fractures, or the tests are terminated at a specified fraction of the measured fracture strain, i.e., at 20%, 40%, 60%, or 80% of the measured fracture strain.
- Step 2. *Delamination testing* of the virgin and damaged paperboards to measure the delamination properties. This reveals how these properties are influenced by damage due to the in-plane straining from the tensile tests in Step 1.

The delamination tests without in-plane straining provide a baseline for further comparisons. Both tensile and ZD testing are performed in a ZwickRoell Z005 testing machine (ZwickRoell; Ulm, Germany).

Tensile loading

The tensile tests are performed similarly to what is stated in ISO 1924-3 “Paper and board — Determination of tensile properties — Part 3: Constant rate of elongation method (100 mm/min),” with the following notable deviations: The width of the specimens and their length are maximized to create the largest possible test specimens for the subsequent delamination tests. This results in a width b = 30 mm and grip-to-grip lengths $L \approx 240$ mm in MD and $L \approx 150$ mm in CD. The elongation rate is maintained at 100 mm/min, as specified in the standard. Due to the change in specimen length, the engineering strain rate is altered from 0.017 s^{-1} in the standard to 0.007 s^{-1} in MD and 0.011 s^{-1} in CD. Consequently, there is approximately a 60% decrease in strain rate in MD and about 35% reduction in the CD tests. This change in strain rate is expected to have a negligible effect on the results. As a rule of thumb, a change in strain rate of one decade of magnitude is needed to influence the strength by roughly 10% (see [22]).

For each paper type, samples of the paperboards are loaded until failure in MD and CD, as well as to 80%, 60%, 40%, and 20% of their fracture strains in CD. **Figure 3** displays the resulting stress-strain curves for these tests. As expected, all paperboard qualities exhibit substantially higher strength in MD than in CD. Additionally, ductility is significantly greater in CD compared to MD. The scatter between individual specimens is minimal. The measured tensile properties indicate that MD strength ranges from 45 MPa to 59 MPa, which is considered a significant variation for boards with similar grammage and thickness. In contrast, the CD strength remains consistent across all boards. The results of the tensile tests are summarized in **Table II**. The data in parentheses represent one standard deviation.

It is observed that some fractured specimens showed local buckling. The buckling appears as a local thickening extending across the width of the specimen and with an axial length of about the thickness of the paperboard. This phenomenon can be attributed to two main factors, as in [23]. First, it is believed to result from an elastic wave propagating from the fracture surface and moving to the grips after the specimen fractures, which can cause localized buckling. Second, the anisotropic nature of the paperboard significantly contributes. These parts of the specimens are rejected for further use. Similarly, parts near the fracture surfaces are also dismissed.

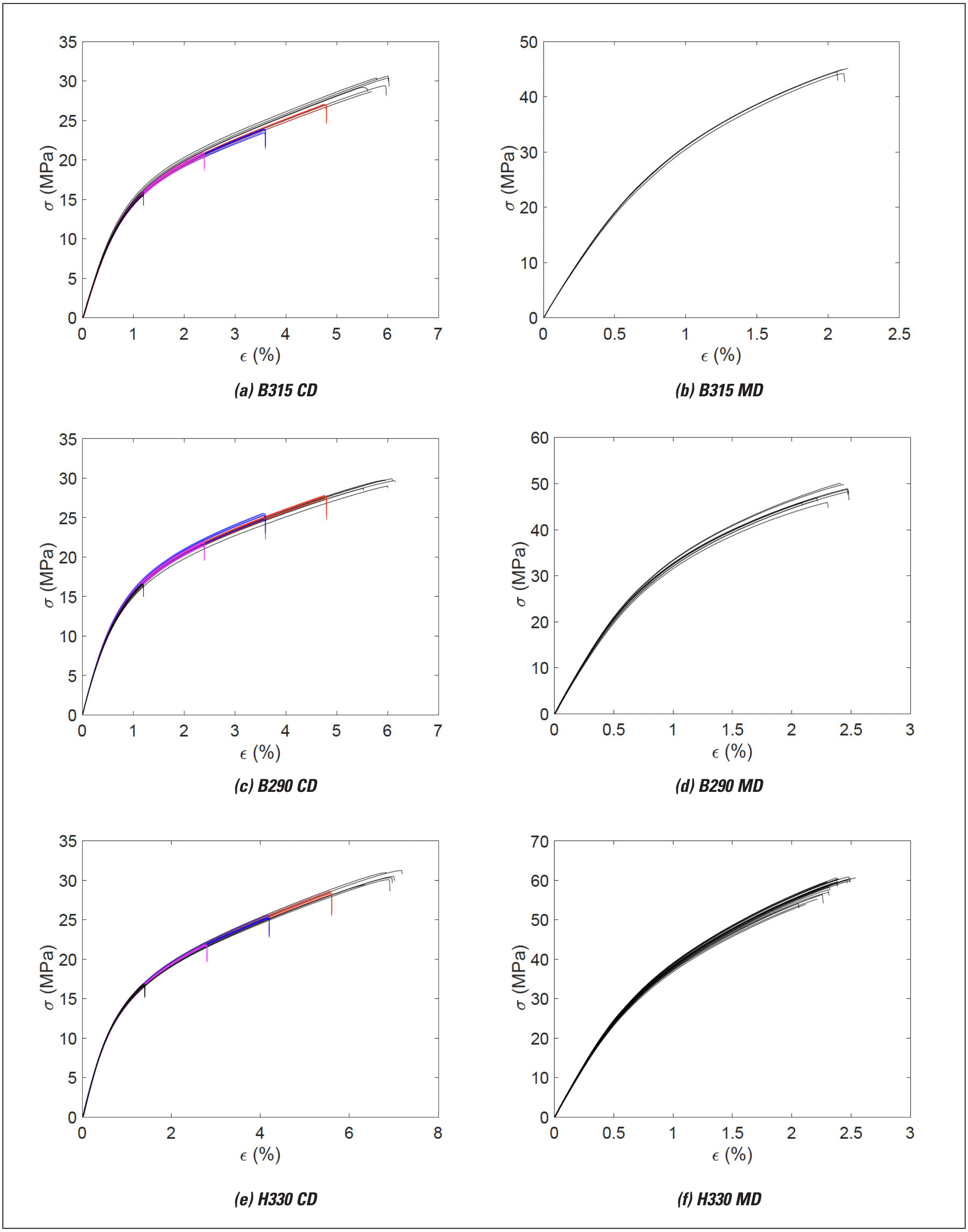

3. Stress-strain plots for in-plane tensile tests. The experiments in the cross-direction (CD) are terminated at five different levels of straining: at fracture, and at 80%, 60%, 40%, and 20% of the fracture strain. In the machine-direction (MD), all experiments are terminated at fracture. Note the difference in stress and strain ranges in the different plots.

Paperboard and Loading Direction	Strain at Fracture, %	Strength, MPa	Young's Modulus, GPa
B315MD	2.1 (0.03)	45 (0.4)	4.3 (0.05)
B315CD	5.9 (0.18)	30 (0.8)	2.2 (0.05)
B290MD	2.3 (0.15)	48 (1.7)	4.7 (0.08)
B290MD	6.0 (0.22)	30 (0.5)	2.5 (0.03)
H330MD	2.3 (0.12)	59 (2.2)	5.5 (0.08)
H330CD	6.9 (0.28)	31 (0.7)	2.3 (0.02)

II. Experimental results from the tensile tests. Numbers in parenthesis are one standard deviation.

ZD tests

The tests in ZD are performed following the TAPPI Standard Test Method T 541. Virgin and damaged paperboard are joined to a specially designed grip (ZwickRoell) using double-coated pressure-sensitive tape, 3M 410M (3M; St. Paul, MN USA). According to the standard, the loading is carried out in two steps. First, the paperboard is compressed to secure the connection to the grips. In the second step, the paperboard is delaminated under a tensile load at the prescribed rate of 66 mm/min. Figure 2 illustrates the test setup.

Repeated tests are performed on each type of paperboard, including virgin paperboard and paperboard strained to fracture in CD and MD. Additionally, tests are conducted on paperboards strained to approximately 80%, 60%, 40%, and 20% of the fracture strain in CD.

Figure 4 shows opening stress σ vs. elongation δ in the z-direction for 13 ZD tests on B315 in its virgin state. We chose to use separation instead of strain in ZD; after the initiation of delamination, opening strain can no longer be derived from the recorded data since the separation includes the effects of the separation of crack surfaces and the straining of the layers. The maximum recorded opening stress, i.e., the strength in ZD, σ_0, is calculated to have the mean value of the strength $\bar{\sigma}_0$ 0.285 MPa. The standard deviation is 0.011 MPa. This value of $\bar{\sigma}_0$, in the virgin state, is used as a base value in the further evaluation of the experimental data for B315. Similarly, the measured values of $\bar{\sigma}_0$ for B290 and H330 are used as base values in the interpretation of the results for these paperboards. The data are summarized in **Table III**. Hence, the experiments on the virgin paperboard showed that the ZD strength of the boards varied from 0.19 MPa to 0.31 MPa. For paperboards, this represents a substantial variation in what can be

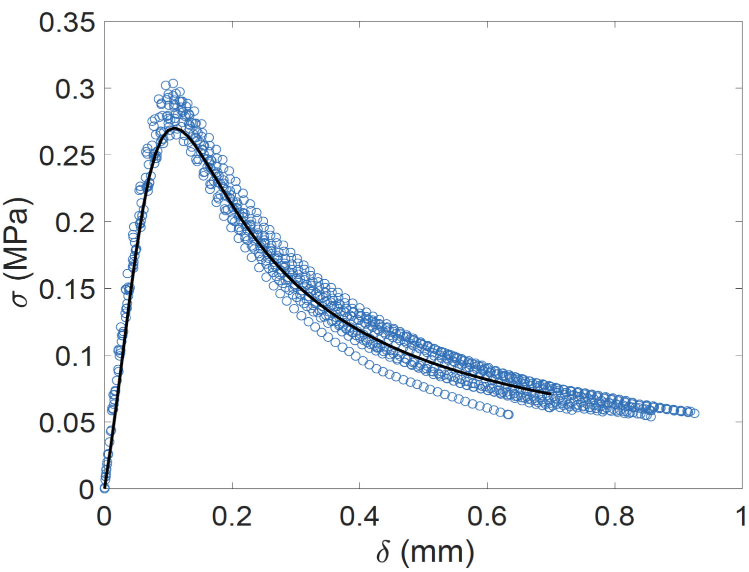

4. Opening stress σ vs. elongation δ in ZD for B315 in its virgin state. The blue circles represent data from the individual ZD-tests, and the black curve is a least-squares fit to the circles according to Eq. 1.

Paperboard and Direction of Pre-Loading	Strain at End of Pre-Loading, %	Plastic Strain at End of Pre-Loading, %	Number of Experiments	ZD Strength, MPa	*K*, MPa/mm
B315V	0	0	13	0.28 (0.01)	3.0
B315CD	1.2	0.5	5	0.29 (0.02)	3.0
B315CD	2.4	1.5	3	0.28 (0.01)	2.4
B315CD	3.6	2.5	3	0.26 (0.008)	2.6
B315CD	4.8	3.6	4	0.25 (0.006)	2.0
B315CD	5.9	4.5	14	0.22 (0.02)	1.8
B315MD	2.1	1.1	10	0.25 (0.03)	2.5
B290V	0	0	15	0.31 (0.02)	3.9
B290CD	1.2	0.5	5	0.32 (0.009)	3.6
B290MD	2.3	1.3	10	0.28 (0.01)	3.3
B290CD	2.4	1.5	5	0.31 (0.006)	3.1
B290CD	3.6	2.6	5	0.29 (0.009)	2.9
B290CD	4.8	3.7	5	0.27 (0.02)	2.4
B290CD	6.0	4.8	15	0.24 (0.01)	2.2
H330V	0	0	15	0.19 (0.01)	6.3
H330CD	1.4	0.7	5	0.20 (0.002)	5.3
H330MD	2.3	1.3	9	0.17 (0.005)	4.5
H330CD	2.8	1.8	5	0.18 (0.004)	4.3
H330CD	4.2	3.1	5	0.16 (0.003)	3.6
H330CD	5.6	4.4	5	0.15 (0.004)	2.6
H330CD	6.9	5.5	14	0.13 (0.005)	1.8

III. Experimental results from ZD-tests. Numbers in parenthesis is one standard deviation. Designation "V" indicates ZD-test performed on paperboard without pre-straining. Plastic strain at the end of pre-loading is calculated from the basic strength-of-material-formula $\epsilon_p = \epsilon - \sigma/E$ and using the relevant value of Young's modulus E from the results of the tensile tests. The out-of-plane stiffness K is derived from curve-fitted data as described in the "ZD tests" portion of the Experimental section.

achieved for multi-ply paperboards.

A rational function is observed to adapt well to the experimental data (Fig. 4):

$$\sigma = \frac{p_1\delta^3+p_2\delta^2+p_3\delta}{\delta^2+q_1\delta+q_2}, \quad (1)$$

It should, however, be noted that the curve is limited to the present values of separation and should not be used for extrapolation. Equation 1 is adapted to the experimental data using the MATLAB CurveFitter application. This is done for all experimental data and for each paperboard type. (It is recognized that alternative methods to determine the free parameters are possible.) It is noted that the adapted curve gives a somewhat smaller strength, i.e., the value $\sigma_0 \approx 0.27$ MPa for B315, than what is directly evaluated from the raw data, i.e., 0.285 MPa for B315. The values of the strength assessed directly from the ZD tests are used in the further evaluation of the experiments.

Of special interest is the elastic stiffness $K = d\sigma/d\delta|_{\delta=0} = p_3/q_2 = 3.02$ MPa/mm for B315 in its virgin state. The data is derived from the adapted rational function. The evaluated values of the stiffness are given in Table III.

RESULTS AND DISCUSSION

The three paperboard grades exhibit similar in-plane properties but differ in z-direction (ZD) modulus and strength (Table III; **Figs. 5–6**). Differences are attributed to ply ar-

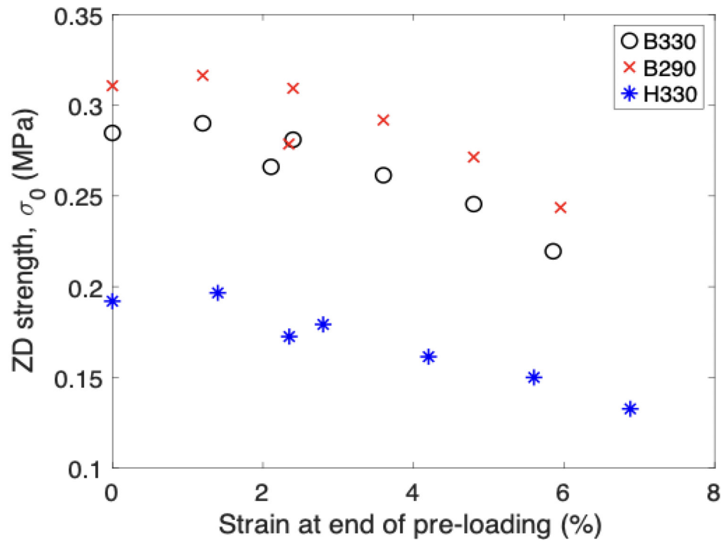

5. Strength in ZD after different levels of pre-straining. Data directly evaluated from the recorded $\sigma(\delta)$*–curves.*

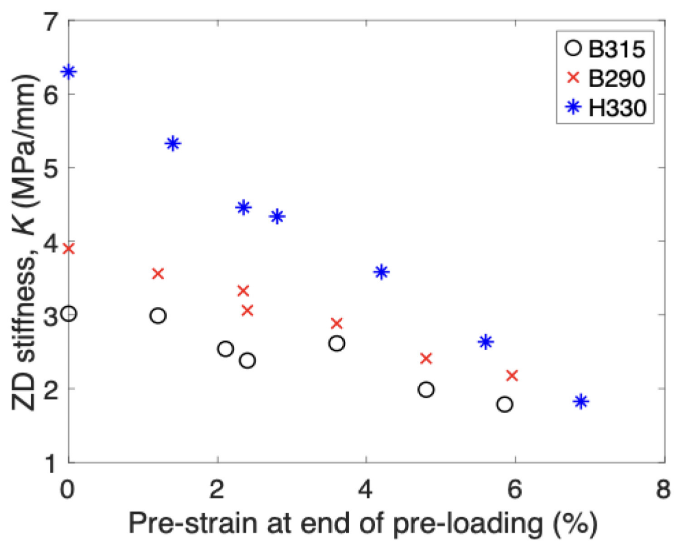

6. Stiffness in ZD after different levels of pre-straining. Data evaluated from the adapted $\sigma(\delta)$*–curves.*

chitecture, fiber orientation, and interfacial bonding. Notably, the grade with the lowest ZD modulus shows comparatively high strength, which can arise when compliant layers arrest or deflect interfacial cracks. At the same time, well-bonded interfaces still carry peak loads. Fractography (**Fig. 7**) indicates that failure predominantly occurs along interfaces, with occasional intra-ply failure. Pre-straining weakens interfacial bonds and shifts the failure locus toward interfaces, explaining the nearly linear reduction in both stiffness and strength with increasing plastic pre-strain.

Figures 8–10 show the adapted rational functions from all experiments on B315, B290, and H330, respectively. It is observed that the pre-straining damages the paperboard. The ZD-tests on 315MD, Fig. 8, do not fully follow the trend indicated by the tests in CD. However, all results from the CD tests appear to result in a gradual decrease in the out-of-plane strength and stiffness with increasing in-plane strain. The results for B290, Fig. 9, are consistent with the results for B315. However, in this case, the results in MD are in better agreement with the trend from the results in CD. For H330, Fig. 10, the results are consistent with the results of the other two paperboards. However, the strength is about 30% smaller than for the two other paperboards.

7. Examples of four fracture surfaces from ZD-tests on B315, i.e., from tests 2, 3, 4, and 5. The paperboard is shown after the ZD-test. It is still fixed to the upper grip, cf. Fig. 2. The surface from test 2 shows an almost uniform structure; test 3 shows about 60% of the surface with a similar color to test 2. However, the rest of the fracture surface is darker. This indicates that the crack path has switched plies during delamination. Test 4 shows an almost uniform, darker surface, and test 5 shows a crack switching plies similarly to test 3.

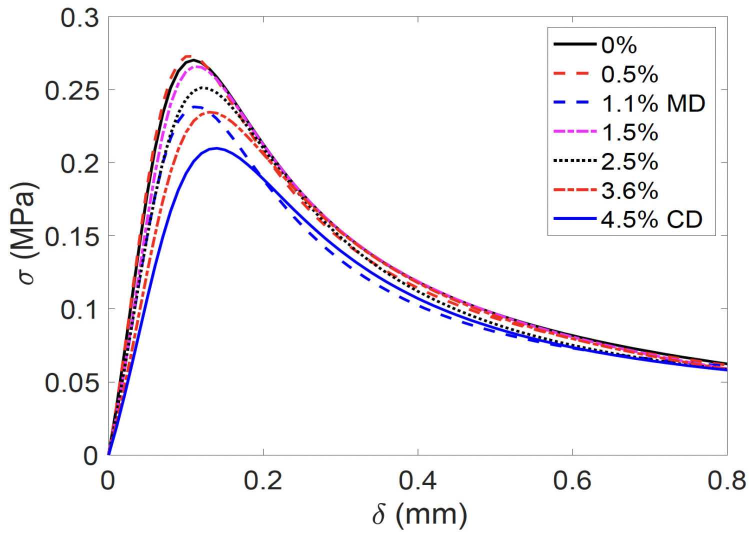

8. Adapted $\sigma(\delta)$–curves for B315 in different damaged states from the virgin state to pre-strained to a plastic strain of 4.5%.

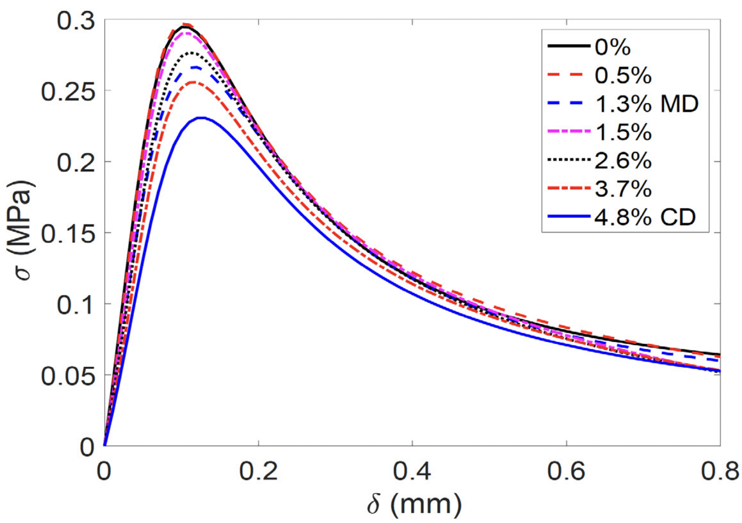

9. Adapted $\sigma(\delta)$–curves for B290 in different damaged states from the virgin state to pre-strained to a plastic strain of 4.8%.

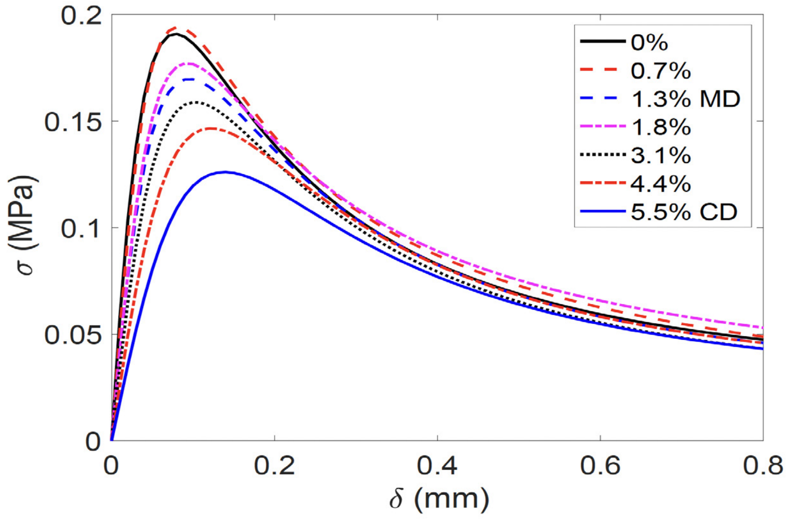

10. Adapted σ(δ)–curves for H330 in different damaged states from the virgin state to pre-strained to a plastic strain of 5.5%.

The influence of the pre-straining on the strength is summarized in **Fig. 11** for all paper grades. A pronounced influence of in-plane straining on the delamination strength of paperboard is shown. It appears to be an almost linear relationship between pre-straining and strength. Effects of pre-straining on the stiffness *K* are shown in Fig. 6. These data show an even larger influence of in-plane straining on *K* as compared to the impact on the strength.

An unexpected result is the slight increase in strength measured with the smallest level of pre-strain, as shown in Fig. 10 and Table III. That is, with about 1% pre-straining corresponding to about 0.5% plastic in-plane strain, all paperboards show a minute increase in strength of about 3%. During small pre-straining, the fibers are pulled and more fiber-fiber bonds are expected to be activated. This would result in a slightly larger strength. A similar phenomenon is reported in [24].

Pre-straining is observed to influence both stiffness and strength almost linearly. A valid assumption is that the damaging effect is uninfluenced by the *elastic* part of the total strain. To this end, we eliminate the elastic strain from the total in-plane strain in the tensile tests and study the influence of the *plastic pre-strain*. Using $\epsilon = \sigma/E + \epsilon_p$ with Young's modulus *E* from the tensile tests, we derive the plastic strain ϵ_p for the tensile tests, as in Table III. It is also interesting to study whether a proper scaling can rationalize the influence; that is, to examine if there is any general property of the results that appears equal between the different qualities of paperboard studied. By introducing the relative reduction in strength, $\Delta\sigma_0/\sigma_0$, we arrive at **Fig. 11**.

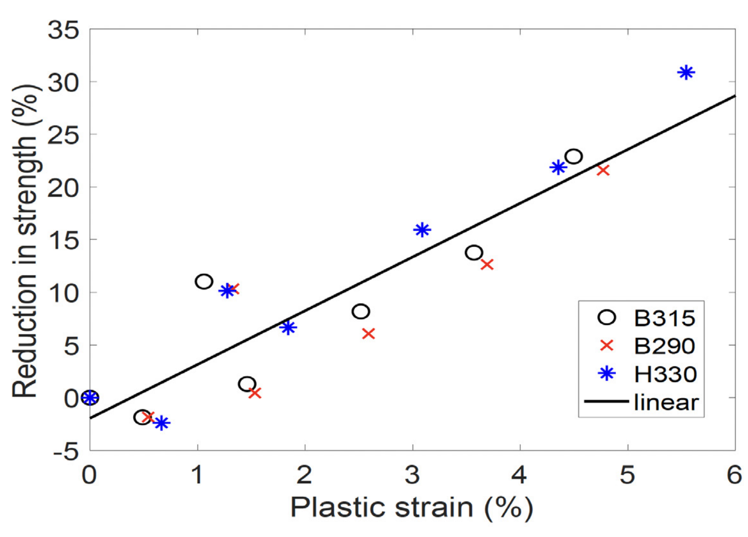

11. Relative reduction in strength from ZD-tests vs. level of plastic pre-straining. The black trend line is a least-squares fit to the data.

The line is a least squares adaptation to all the data points. It is noted that the adapted line well approximates the data:

$$\frac{\Delta\sigma_0}{\sigma_0} = -0.020 + 0.051\epsilon_p \quad (2)$$

If this is a general result, it would drastically reduce the need for experimental studies. Instead of being forced to evaluate each paper type at several strain levels, only the virgin state would suffice, and Eq. 2 can be used to *predict* the influence of in-plane straining on the ZD strength of paperboard.

Figure 12 shows a plot of the influence of plastic pre-straining on the out-of-plane stiffness *K*. A least squares adaptation gives the relative reduction of stiffness as:

$$\frac{\Delta K}{K_0} = 0.027 + 0.10\epsilon_p \quad (3)$$

where K_0 is the stiffness for the virgin material, as given in Table III. Thus, the influence of plastic in-plane straining is about twice as large on the stiffness than on the strength. The result suggests that only the virgin state of the paperboard needs to be tested, and Eq. 3 can be used to predict the influence of pre-straining on *K*.

As shown, both the ZD stiffness and the strength of the paperboard are reduced due to in-plane straining. This has potential implications for delamination during the creasing process where the paperboard is sheared. If similar reductions in strength and stiffness are observed in shear, the effects on delamination during creasing are not obvious. The lower stiffness gives smaller stresses, and the lower strength makes delamination possible with smaller stresses. However, the effect of plastic straining on the stiffness is about twice as large as its effect on the strength (Eq. 2 and Eq. 3). That is, it is not obvious how this effect affects the creasing and folding processes. This topic needs further research.

All paperboards in this study are manufactured in continuous industrial processes. These processes result in uneven distributions in fiber orientation with fibers mainly orientated in the plane of the paper. Primarily in MD, however, fibers are also oriented towards the cross direction, CD. As a result, the Young's modulus in MD is about twice as large as observed in CD (Table II).

The distribution in fiber orientation also helps us understand the observed dramatic differences in strain-to-failure as noted in the tests [22]. Table II shows almost three times larger strain-to-failure in CD than in MD. In ZD, the "engineering strain" to failure δ_{max}/t is orders of magnitude larger than the strain-to-failure in in-plane loading. (In the ZD tests, the experiments were chosen to be terminated when the stress in ZD had decreased to 80% of the maximum stress.) It should be noted that the meaning of strain is lost after the delamination starts. With the paperboard split by a delamination crack, the total separation is the sum of the effects of a crack opening and the straining of the layers above and below the delamination crack.

During in-plane plastic straining, fiber bounds fail [14]. This is believed to be a main reason for the loss in ZD stiffness and strength. The larger the plastic strain, the larger is the decrease in both stiffness and strength. Moreover, it appears that the damaging effect of plastic straining is independent of the direction of straining. That is, the same amount of plastic strain in MD and CD gives similar effects on the ZD strength and stiffness.

In [25], the fibers are shown to reorient with the straining of paperboard in CD. That is, the fibers orient in the straining direction. No such effect could be quantified in MD. However, with alignment of the fibers in the plane of the paperboard, fewer fiber bonds need to break in ZD

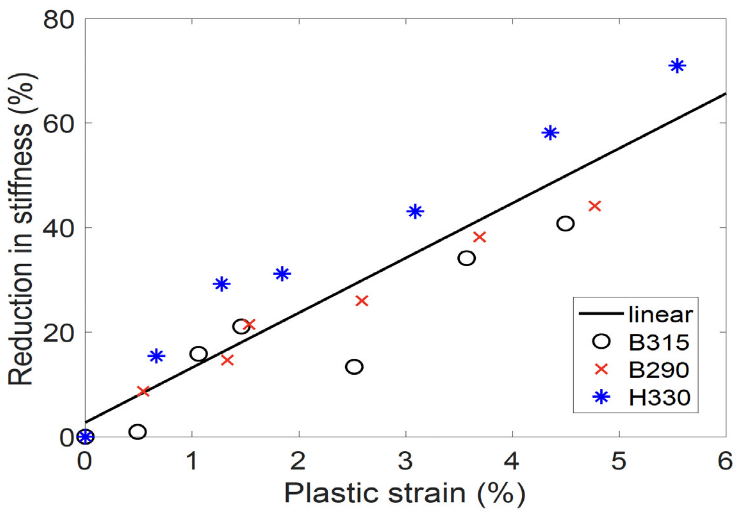

12. Relative reduction in stiffness from ZD-tests vs. level of plastic pre-straining. The black trend line is a least-squares fit to the data.

loading, and smaller strength would be expected in ZD with fiber reorientation. This might be an additional mechanism behind the results shown in the present study.

One of the paperboards, B315, showed slightly different behavior than the other two. In pre-strained states, B315 showed fracture surfaces in two different colors (Fig. 7). This is believed to be due to two potential crack paths with similar strengths. A crack at the interface between two layers can jump to a weaker, competing interface. This matches the observed two-colored fracture surface in test 3 in Fig. 7. Conversely, tests 2 and 4, which had the same pre-strain, show cracks growing along only one interface, indicating that both crack paths are equally probable. This probably explains why B315 behaves somewhat differently from B290 and H330, as seen in Figs. 4, 8, and 9.

CONCLUSIONS

The experiments demonstrate that in-plane plastic straining significantly reduces out-of-plane stiffness and delamination strength of paperboard. These effects are primarily attributed to the weakening of interfacial bonds, as confirmed by observations of the fracture surface. While absolute values differ between grades, the relative reduction in stiffness and strength with plastic pre-strain appears nearly linear and similar across the studied grades.

The present study applied in-plane straining before ZD testing; potential coupling effects of simultaneous loading modes are a topic for future studies. If the observed trends generalize, they could substantially reduce the need for extensive experimental campaigns when characterizing paperboard for converting processes. The industrial implications are as follows:

- Virgin-state ZD tests may be sufficient to establish predictive relationships for stiffness and strength reduction as a function of plastic pre-strain, thereby reducing the experimental workload.
- Tooling and fixation strategies can be optimized to minimize in-plane plasticity during creasing and folding.
- Process simulations should incorporate the sensitivity of ZD properties to pre-straining to improve predictions of crease quality and surface crack risk.

Looking ahead, these findings provide a foundation for implementing a Digital Twin paradigm in paperboard converting and forming into boxes. By embedding the predictive relationships developed here into a virtual replica of the creasing and folding process, a digital twin could enable real-time monitoring of in-plane strain, simulate ZD property degradation, and optimize process parameters. Such an approach would support predictive maintenance, reduce waste, and accelerate the transition toward data-driven, Industry 4.0-enabled packaging operations.

ACKNOWLEDGEMENT

This study is part of the research project Characterisation of Paperboard for Creasing and Folding (CPCF) financed in part by the Knowledge Foundation, Sweden, Tetra Pak Packaging Solutions AB, Billerud Sweden AB, and Holmen Iggesund Paperboard AB. The CPCF is a joint project involving Örebro University and the industrial partners. Support from all partners is gratefully acknowledged.

LITERATURE CITED

1. Coffin, D. and Nygårds, M., "Creasing and folding," in *Advances in Pulp and Paper Research, Oxford 2017, Trans. of the XVIth Fund. Res. Symp. Oxford, 2017*, (W. Batchelor and D. Söderberg, Eds.), pp. 69–136, FRC, Manchester, 2018. https://doi.org/10.15376/frc.2017.1.69.
2. Timoshenko, S.P. and Gere, J.M., *Theory of Elastic Stability*, McGraw-Hill, New York, 1961.
3. Carlsson, L., De Ruvo, A., and Fellers, C., *J. Mater. Sci.* 18: 1365(1983). https://doi.org/10.1007/BF01111956.
4. Beex, L. and Peerlings, R., *Int. J. Solids Struct.* 46(24): 4192(2009). https://doi.org/10.1016/j.ijsolstr.2009.08.012.
5. Nygårds, M., Just, M., and Tryding, J., *Int. J. Solids Struct.* 46(11): 2493(2009). https://doi.org/10.1016/j.ijsolstr.2009.02.014.
6. Xia, Q.S., Boyce, M.C., and Parks, D.M., *Int. J. Solids Struct.* 39(15): 4053(2002). https://doi.org/10.1016/S0020-7683(02)00238-X.
7. Giampieri, A., Perego, U., and Borsari, R., *Int. J. Solids Struct.* 48(16): 2275(2011). https://doi.org/10.1016/j.ijsolstr.2011.04.002.
8. Borgqvist, E., Wallin, M., Tryding, J., et al., *Compos. Struct.* 126: 184(2015). https://doi.org/10.1016/j.compstruct.2015.02.067.
9. Li, Y., Stapleton, S.E., Reese, S., et al., *Int. J. Solids Struct.* 130-131: 172(2018). https://doi.org/10.1016/j.ijsolstr.2017.10.003.
10. Simon, J.-W., *Arch. Comput. Methods Eng.* 28: 2409(2021). https://doi.org/10.1007/s11831-020-09460-y.
11. Robertsson, K., Borgqvist, E., Wallin, M., et al., *Packag. Technol. Sci.* 31(8): 557(2018). https://doi.org/10.1002/pts.2383.
12. Robertsson, K., Borgqvist, E., Wallin, M., et al., *Appl. Math. Model.* 99: 497(2021). https://doi.org/10.1016/j.apm.2021.07.005.
13. Alzweighia, M., Tryding, J., Mansour, R., et al., *J. Mech. Phys. Solids* 181: 105430(2023). https://doi.org/10.1016/j.jmps.2023. 105430.
14. Borodulina, S., Kulachenko, A., Galland, S., et al., *Nord. Pulp Pap. Res. J.* 27(2): 318(2012). https://doi.org/10.3183/npprj-2012-27-02-p318-328.
15. Gradin, P., Graham, D., Nygård, P., et al., *Exp. Mech.* 48(1): 133(2008). https://doi.org/10.1007/s11340-007-9055-7.
16. Hägglund, R. and Isaksson, P., *Int. J. Solids Struct.* 45(3-4): 868(2008). https://doi.org/10.1016/j.ijsolstr.2007.09.011.
17. Page, D.H. and El-Hosseiny, F., *J. Pulp Pap. Sci.* 9(4): 99(1983).
18. Räisänen, V.I., Alava, M.J., Nieminen, R.M., et al., *Nord. Pulp Pap. Res. J.* 11(4): 243(1996).
19. Seth, R.S. and Page, D.H., "The stress strain curve of paper," in *The Role of Fundamental Research in Paper-Making, Trans. of the VIIth Fund. Res. Symp. Cambridge, 1981*, (Fundamental Research Committee, Ed.), pp. 421–452, FRC, Manchester, 2018. https://doi.org/10.15376/frc.1981.1.421.
20. Biel, A., Tryding, J., Ristinmaa, M., et al., *Int. J. Solids Struct.* 252: 111755(2022). https://doi.org/10.1016/j.ijsolstr.2022.111755.

21. Ebrahimijamal, I., Biel, A., Tryding, J., et al., *Exp. Mech.* 65: 1147(2025). https://doi.org/10.1007/s11340-025-01204-y.

22. Poddar, S., Andreasson, E., and Nygårds, M., *Nord. Pulp Pap. Res. J.* 39(3): 349(2024). https://doi.org/10.1515/npprj-2024-0012.

23. Johnson Jr., M.W. and Urbanik, T.J., *Wood Fiber Sci.* 19(2): 135(1987).

24. Marin, G., Nygårds, M., and Östlund, S., *Packag. Technol. Sci.* 35: 69(2022). https://doi.org/10.1002/pts.2608.

25. Johansson, S., Engqvist, J., Tryding J., et al., *Strain* 58(5): e12414(2022). https://doi.org/10.1111/str.12414.

ABOUT THIS PAPER

Cite this article as:
Stigh, U., Biel, A., Tryding, J., et al., *TAPPI J.* 25(3): 180(2026). https://doi.org/10.32964/TJ25.3.180

DOI: https://doi.org/10.32964/TJ25.3.180

ISSN: 0734-1415

Publisher: TAPPI Press

About this journal

ABOUT THE AUTHORS

We studied this topic because we are curious about the mechanical properties of materials, how the microstructure influences these properties, and how they can be described mathematically. The properties we have measured in this study have up until now been assumed to be uninfluenced by in-plane straining. We show that there is a surprisingly large influence.

Our biggest challenge was finding a way to perform the experiments with standard equipment. It was most surprising to find that the influence of in-plane straining can be captured in simple formulas that appear independent of the specific paperboard.

The complete consequences of the discoveries here are not understood at this moment but warrant further study. Currently, we are performing shear tests.

Stigh is guest professor and Biel is senior lecturer in the Department of Engineering and Physics at the University of Karlstad, in Karlstad, Sweden. Tryding was a senior specialist in Materials at Tetra Pak Packaging Solutions AB in Lund, Sweden. Nygårds is a specialist in Paper Physics and Converting at Billerud AB in Solna, Sweden. Vomhoff is project manager at Holmen Iggesund Paperboard in Iggesund, Sweden. Persson and Korin are associate professors and Karlsson is senior lecturer at Örebro University in Örebro, Sweden. Email Stigh at ulf.stigh@kau.se.


Stigh


Biel


Tryding


Nygårds


Vomhoff


Persson


Korin


Karlsson